3rd URSI AT-AP-RASC, Gran Canaria, 29 May – 3 June 2022

Satellite attitude effects on the reception of transionospheric HF signals: Examples from the Radio Receiver Instrument onboard e-POP/Swarm-E

E. C. K. Eyiguler * (1,2), D. W. Danskin (1), G. C. Hussey (1), K. Pandey (1), R. G. Gillies (3), A. W. Yau(3)
(1) University of Saskatchewan, Institute of Space and Atmospheric Sciences, Saskatoon, SK, CA, http://www.usask.ca
(2) Istanbul Technical University, Meteorological Engineering, Istanbul, TR
(3) Department of Physics and Astronomy, University of Calgary, Calgary, Alberta, Canada

Abstract

The characteristics observed by an antenna onboard a spacecraft depend on the geometry between the receiving antenna and the electric fields of the radio wave. The antenna boresight direction should be along the transmitting source's line-of-sight direction to be able to completely resolve the wave's polarization characteristics. However, this is not always the case, especially for the antenna onboard a spacecraft due to the spacecraft orientation restrictions. Hence, in this study, the focus is on the antenna orientation effects on the observed polarization characteristics of the radio wave. Precise quaternion and sp3 orbit data of Swarm-E (formerly known as the CAScade, Smallsat, and Ionospheric Polar Explorer – CASSIOPE) spacecraft are used to determine the boresight of the Radio Receiver Instrument (RRI) onboard, for the coordinated experiments with the NRCAN-Ottawa transmitter (45.4°N, 75.6°W). The observed characteristics of the HF radio waves are determined for two selected cases with different attitude behavior: slew-to-target on 14 May 2017, and nadir mode on 11 August 2017. The effect of the angle between dipoles and radio wave propagation direction should be removed to resolve the physical characteristics of the wave.

1. Introduction

Swarm-E, previously known as the CASSIOPE (CAScade, Smallsat, and Ionospheric Polar Explorer) before joining the Swarm team in 2018, is a satellite with 81° inclination in elliptical-polar orbit [1]. Swarm-E is equipped with the e-POP scientific suite, which carries multiple scientific instruments for the in-situ observations of the ionosphere. One of these instruments is the Radio Receiver Instrument (RRI). RRI has two 6-m dipoles, arranged orthogonal to each other to form cross-dipoles for the investigation of radio wave characteristics. RRI bandwidth ranges from 10 Hz to 18 MHz [2]. RRI measures the complex voltages induced on each dipole during the experiments. The source of the induced voltages, that is, the received signal, can be either man-made or pertaining to natural sources [3].
Previously, some of the coordinated experiments between the RRI and terrestrial transmitters on the ground were with Sura [4], SuperDARN [5], European Incoherent Scatter HF facility in Tromsø, Norway [6], and the NRCAN-Ottawa transmitter [7] for the investigations of radio wave characteristics [5, 7], direction of arrival [6] and ionospheric structures and irregularities [4].
The polarization characteristics of the wave can be calculated by utilizing the general Stokes parameters [8, 9] assuming that the signal is following the line-of-sight path from the transmitter to the spacecraft and the wave electric field projects itself fully onto the dipole plane. For the latter, the dipoles should be in the plane perpendicular to the propagation path of the radio wave. For the slew-to-target coordinated experiments of the RRI, this condition is nearly satisfied. However, in practice there are small deviations from the perfect slew due to maneuvering constraints of the satellite and inaccuracies in star-sensor and magnetometer measurements for the spacecraft attitude determination [10].
Consequently, in this work, two coordinated experiments are presented between the e-POP RRI and Ottawa transmitter. In the first experiment on 14 May 2017, RRI slewed towards the ground target. The second experiment, 11 August 2017, is an example of a Nadir-pass where the RRI boresight was along the satellite trajectory.

2. Data and Methodology

The ePOP/Swarm-E spacecraft body reference frame was constructed such that the RRI boresight is along the X axis, the Suprathermal Electron Imager (SEI) boom is on the Y axis and the Fast Auroral Imager (FAI) CCD cameras are on the Z axis. In orbital reference frame, Z looks downward in the Nadir direction; Y is along the negative orbit normal and X is along the ram direction. This configuration is defined as the Nadir mode of the spacecraft [11].
During the slew-to-target experiments, X is aligned such that it points towards the target on the ground. However, the accuracy of pointing varies due to the satellite attitude. Attitude accuracy of the Swarm-E can typically range from 30 arcseconds to 200 arcseconds, depending on the orientation of satellite and the available attitude sensors, and are provided in the quaternion file [12].
Additionally, the precise knowledge of the spacecraft position is a necessity in the calculation of the line-of-sight (LOS) ray vector from the ground to the spacecraft. One

advantage of the Swarm-E is that precise Standard Product #3 (sp3) format [13] data is available for the spacecraft position.

In this work, the quaternion and sp3 data files are needed to calculate the RRI boresight pointing direction and the LOS ray vector. Both files are available online on the e-POP website [14]. The LOS ray vector is computed using the spacecraft and transmitter locations throughout the trajectory. Boresight angle is defined as the angle between the boresight direction and the LOS ray vector. It is calculated by utilizing the quaternions and tracks the change in the X axis' pointing direction. Dipole observation angle is the angle between the maximum gain direction of a dipole and the ray vector. Lastly, aspect angle is defined as the angle between the magnetic field and the ray vector. The polarization characteristics of the observed wave, such as the powers at each dipole, the orientation angle, and the ellipticity angle were calculated via the Stokes parameters as shown in [7].

For the purposes of the present study, two experiments were selected according to their attitude behavior, the transmitter frequency and the ionospheric characteristics during the pass. The first experiment on 14 May 2017 is an example of slew-to-target pass, whereas the experiment on 11 August 2017 is an example of a Nadir pass. During the slew-to-target pass, the spacecraft traveled from Southwest to Northeast. On the other hand, during the Nadir pass, the spacecraft traveled from Southwest to Northeast. Both days were geomagnetically quiet. The transmitting radar frequency for each event was 8.0995 MHz. The transmitted signal was composed of a Continuous Wave (CW) and a Binary Phase Shifted Key (BPSK) part. The CW part lasted for 0.9 seconds, starting at each 10 second and BPSK part lasted for 7 seconds starting 1.1 second after the end of each CW transmission [7]. Other than the differences in their type of orbits, these experiments were specifically selected for the close timing of the spacecraft passages and the similarity in their ionospheric characteristics, such as the F-region peak plasma frequency (foF2) and its altitude (hmF2). The start time of the experiments were 17:04 and 16:20 UTC, respectively, which correspond to 12:04 and 11:20 Local Time, around local noon. Ionospheric parameters during the passes were obtained from the DIDBASE, GIRO web portal (https://giro.uml.edu/didbase/). foF2 was 5.3 MHz for the 14 May pass and was 4.6 MHz during the 11 August pass. hmF2 values were the same and were 210 km.

3. Results

Figure 1 shows the RRI cross-dipole configuration and observed wave's characteristics for the 14 May 2017 pass. On the left hand-side of the figure, 3D properties of the pass are presented in geographic coordinates. The figure is

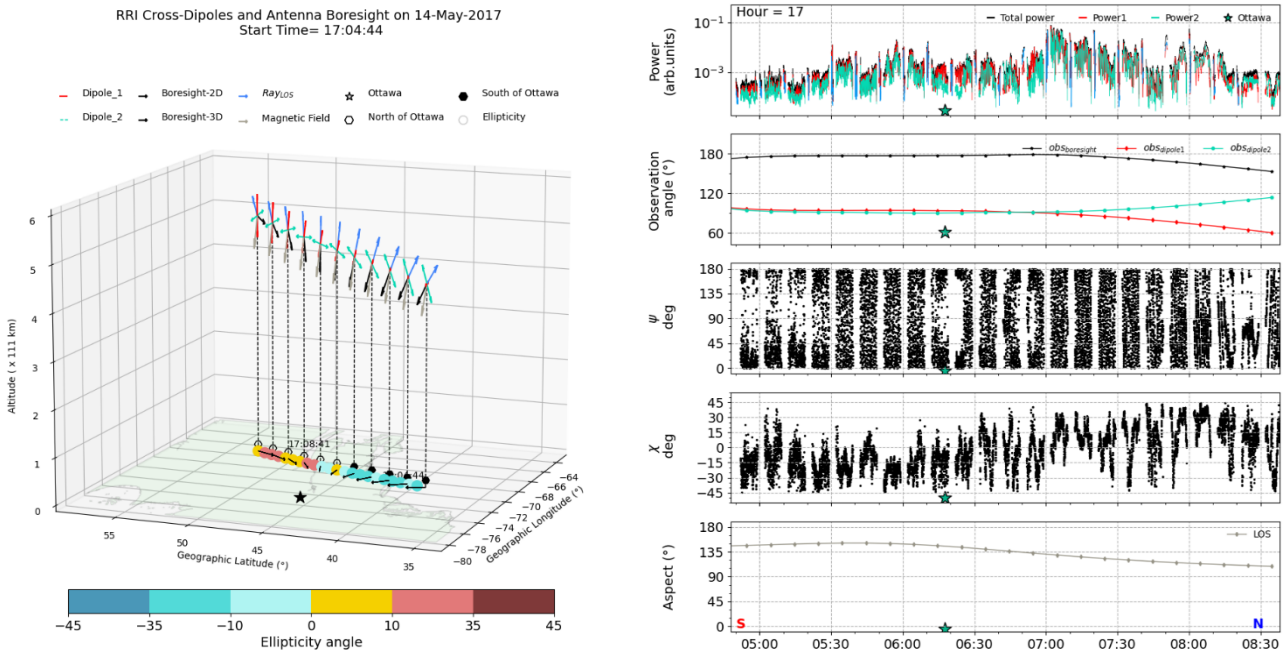

Figure 1: RRI cross-dipole configuration and observed wave's polarization characteristics for the slewed pass. The left panel: 3D view of the spacecraft trajectory and RRI cross-dipole configuration (dipole1 depicted in red, dipole 2 in green); 3D vectors of the RRI pointing vector, the line-of-sight ray vector, and the magnetic field vector in black, blue and grey respectively. On the ground projection: RRI 2D pointing vector depicted in black, ellipticity angles averaged throughout the BPSK sequence are shown as colored circles. On the right: the first panel shows the total power and the powers observed at each dipole; the right panel, the observation angle of dipole1 (red), dipole2 (green), and RRI boresight (black); the third panel, the orientation angle; the fourth panel, the ellipticity angle; and lastly, the fifth panel, the aspect angle. Hour of the pass (17 UTC) is given on the top left. On the bottom right, S and N denote the south and north of Ottawa, and location of Ottawa is shown with a green star in each panel.

slightly tilted to show the vectors more clearly. In the figure, RRI boresight is denoted with black arrows in 3D and its 2D projection on the ground. As evident from the left hand-side of the figure, RRI was slewing towards Ottawa throughout the pass. The ray vector, denoted in blue, showed that RRI received the signal from its front during the passage. Dipole1, shown in red and dipole2, shown in green were rotating in 3D to slew towards the ground target. The ellipticity angle, which was averaged over the BPSK sequences, show left-hand circular (negative) ellipticity in the South part of the pass. In the northern part of the passage, the ellipticity of the wave displays right-hand circular (positive) values. However, the actual behavior of the ellipticity angle was much more complicated and variable during the sequences.

Observed polarization parameters of the wave are presented on the right hand-side of Figure 1. In the first panel power received at dipole1, dipole 2 and the total power are given in red, green and black colors, respectively. Powers displayed similar orders of magnitude for the most of the pass and the total power was oscillating between the two dipoles. This result is expected for the slew-to-target passages, which show that the dipoles were capturing the signal almost equally. The second panel in the figure displays the calculated boresight and dipole observation angles for this pass. When the boresight angle is 180º, it means that the RRI is receiving the signal from its front, and is coplanar to the electric field of the polarized signal. When the boresight angle is below 90 º and heading towards 0º, this shows that the RRI is receiving the signal from its back. On the other hand, for a dipole to best observe the electric field of the incident wave, the dipole observation angle should be 90º. As seen, the boresight angle of the RRI was almost equal to 180º until 17:07:10 UTC for the 14 May 2017 experiment, showing that this was an almost perfectly slewed pass. After 17:07:10, the boresight angle slowly started to deviate from the line-of-sight path connecting the transmitter to the RRI. At the end of the passage the deviation from the LOS became as large as 40º. Similarly, observation angles for dipole1 and dipole2 were very close to 90º in the beginning, and started to show deviations after 17:07:10. Maximum deviations were around 30º and -30º for dipole1 and dipole2, respectively.

The third panel shows the observed orientation angle variations during the 14 May 2017 experiment. In the beginning of the passage, the orientation angle varied smoothly from 180º to 0º with repetitions due to phase wrapping as a consequence of Faraday rotation. Later, a reversal in the Faraday rotation occurred in the Northern side of the pass at 17:08:30 and the variations changed to the opposite sense, ranging from 0º to 180º. In [7], the authors also observed the Faraday reversals in the Northern part of the slewed passages.

The ellipticity angle in the fourth panel shows that, despite, the averaged over the BPSK values were pretty smoothly behaving, there were large variations in the ellipticity during the individual sequences. Northward of Ottawa, the variations became larger, changing from left-hand-circular to linear, than to right-hand circular.

Figure 2 displays the properties of the Nadir pass on 11 August 2017, in the same format as Figure 1. During this pass, the RRI boresight was along the ram direction and the dipoles lied in the y-z plane, unchanging their position. Due to this behavior, RRI received the signals from its front until its closest approach to Ottawa at 16:21:30. After that time, RRI started to receive the signals from its back. As the Nadir pass is a descending pass, the ellipticity angle behavior is the opposite of the slewed case in Figure 1. As the satellite traversed the region, the average ellipticity angle varied from left circular at the beginning, to linear near the center, and to right circular at the end of the pass.

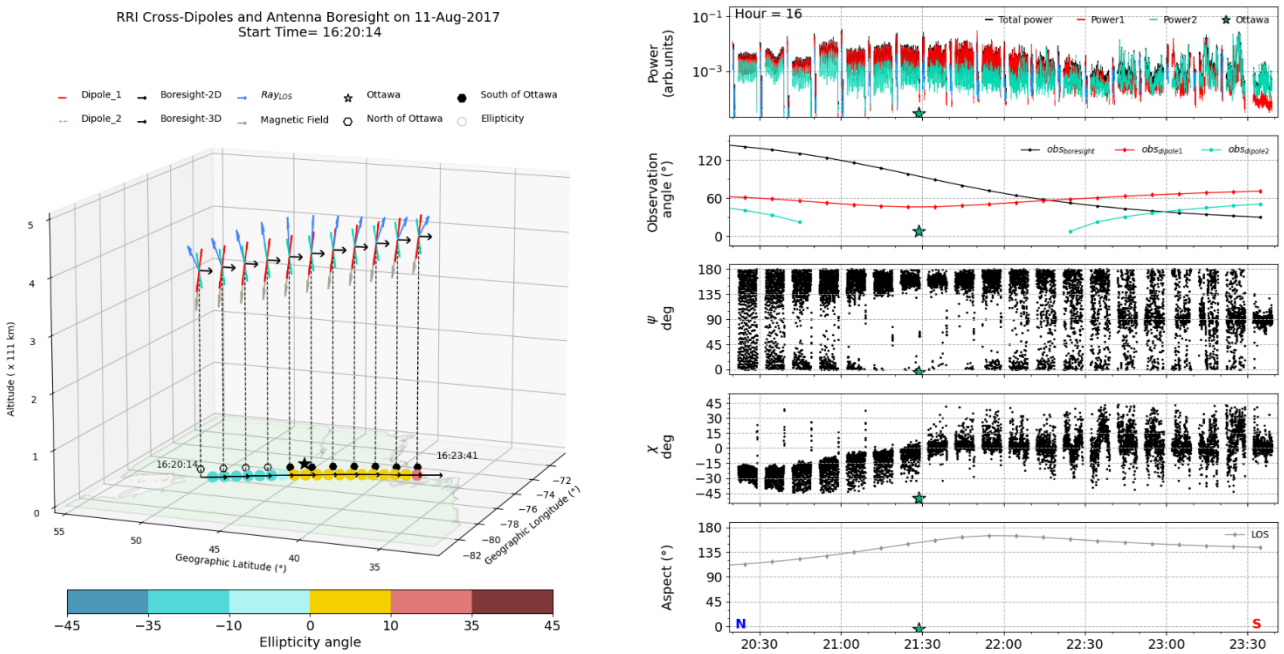

Figure 2: Same as Figure 1, but for the 11 August 2017, Nadir pass.

Additionally, unlike the slewed pass, in which almost equal order of magnitude powers were observed, in the Nadir pass, the power at dipole 2 was half of dipole 1. As a result, the total power was much closer to the power at dipole 1 since it was the dominant observing dipole. The second panel presents the reasons of this behavior. The observation angle of dipole2 dropped to zero and had a discontinuity between 16:20:30 UTC and 17:22:20 UTC. This is because the dipole 2 was receiving the signal from one of its ends and it was not able to observe any component of the electric field. Nonetheless, dipole1 was still partially oriented towards the transmitted signal, although, its observation angle varied between ~45º and ~75º. Accordingly, dipole 1 observed some part of the signal and not all components of the electric field. As a consequence, the orientation angle varied only between 135º and 180º. No Faraday reversals were observed during this event. On the other hand, the aspect angle reached ~180º in the middle of the pass. Theoretically, linear waves are expected when the aspect angle is close to 180º. However, since, only dipole 1 was receiving the signal with 45º observation angle and seeing only a part of the signal that is incident on its plane, the variations in the ellipticity angle were much broader during the individual sequences.

4. Summary and Discussion

In this study, the observed polarization characteristics of the waves at RRI onboard e-POP/SWARM-E were presented for two cases, one slew-to-target experiment on 14 May 2017, and one Nadir pass experiment on 11 August 2017. Different behaviors in the ellipticity and orientation angles were observed during the passes despite the ionospheric parameters being very similar for the two experiments. The results suggest that the variations in the observed polarization parameters, especially the range of variations in the orientation angle and the respective order of magnitude power at each dipole, depend on the observation angle of the individual dipoles, and the antenna boresight. The observation angle is a key parameter necessary for explaining if the dipole plane is able to measure the total electric field of the polarized wave. The next step is to eliminate the effects of dipole orientation during the experiments, so that the 'actual' electric field and 'true' polarization characteristics of the radio wave can be approximated with high accuracy.

5. Acknowledgements

We gratefully acknowledge the funding support from the European Space Agency, MacDonald Dettwiler and Associates, the Canadian Space Agency, the Industrial Technologies Office and the Natural Science and Engineering Research Council (NSERC) for the development of the CASSIOPE mission, and operation of the CASSIOPE spacecraft, including the Cascade and e-POP payloads. Specifically, we acknowledge the support of the ESA and CSA [21SUSTTRRI] for the present study. We also thank the DIDBASE, GIRO data providers.

References

[1] Yau, A. W., & James, H. G. (2015). CASSIOPE enhanced polar outflow probe (e-POP) mission overview. *Space Science Reviews*, *189*(1), 3-14

[2] James, H. G., King, E. P., White, A., Hum, R. H., Lunscher, W. H. H. L., & Siefring, C. L. (2015). The e-POP Radio Receiver Instrument on CASSIOPE. Space Science Reviews, 189(1–4), 79–105. . https://doi.org/10.1007/s11214-014-0130-y

[3] Maxworth, A., Hussey, G., & Gołkowski, M. (2020). Coexistence of Lightning Generated Whistlers, Hiss and Lower Hybrid Noise Observed by e-POP (SWARM-E)–RRI. *Atmosphere* 2020, Vol. 11, Page 177, 11(2), 177. https://doi.org/10.3390/ATMOS11020177

[4] James, H. G., Frolov, V. L., Andreeva, E. S., Padokhin, A. M., & Siefring, C. L. (2017). Sura heating facility transmissions to the CASSIOPE/e-POP satellite. Radio Science, 52(2), 259–270. https://doi.org/10.1002/2016RS006190

[5] Perry, G. W., Frissell, N. A., Miller, E. S., Moses, M., Shovkoplyas, A., Howarth, A. D., & Yau, A. W. (2018). Citizen radio science: An analysis of amateur radio transmissions with e-POP RRI. *Radio Science*, 53, 933– 947. https://doi.org/10.1029/2017RS006496

[6] James, H. G. (2018). Propagation Directions of High-Frequency Waves in the Ionosphere. Radio Science, 53(4), 440-447. https://doi.org/10.1002/2017RS006474

[7] Danskin, D. W., Hussey, G. C., Gillies, R. G., James, H. G., Fairbairn, D. T., & Yau, A. W. (2018). Polarization Characteristics Inferred from the Radio Receiver Instrument on the Enhanced Polar Outflow Probe. *Journal of Geophysical Research: Space Physics*, *123*(2), 1648–1662. https://doi.org/10.1002/2017JA024731

[8] Born, M., &Wolf, E. (1980). Principles ofoptics: Electromagnetic theory ofpropagation, interference and diffraction oflight (6th ed.). Oxford, UK: Pergamon Press.

[9] Hussey, G. C. (1994). The polarisation of 50 MHz auroral backscatter, (PhD thesis). Saskatoon, Saskatchewan: University of Saskatchewan.

[10] Siemes, C. (2019). *TECHNICAL NOTE: CASSIOPE Star Sensor Attitude Data Combination*. https://swarm-diss.eo.esa.int/?do=download&file=swarm%2F%23CASSIOPE_e-POP%2FPrecise_Attitude_Data%2FESA-EOPSM-SWRM-TN-3487.pdf

[11] (2022, 10 January). CASSIOPE SPACECRAFT (Swarm-E) PROCESSED DATA HANDBOOK, Coordinate systems: https://epop.phys.ucalgary.ca/data-handbook/coordinate-systems/.

[12] (2022, 10 January). CASSIOPE SPACECRAFT (Swarm-E) PROCESSED DATA HANDBOOK, Attitude Quaternion File (CAS_AttQuat), https://epop.phys.ucalgary.ca/data-handbook/attitude-quaternion-file-cas_attquat/

[13] Spofford, P. R., & Remondi, B. W. (1994). The national geodetic survey standard GPS format SP3. *SP3-a format) available from the IGS website: http://igscb.jpl.nasa.gov/igscb/data/format/sp3_docu.txt*

[14] (2022, 10 January). e-POP data: https://epop.phys.ucalgary.ca/data/